

Noé Jiménez

Olga Umnova

Jean-Philippe Groby *Editors*

Acoustic Waves in Periodic Structures, Metamaterials, and Porous Media

From Fundamentals to Industrial
Applications

Topics in Applied Physics

Volume 143

Series Editors

Young Pak Lee, Physics, Hanyang University, Seoul, Korea (Republic of)

David J. Lockwood, Metrology Research Center, National Research Council of Canada, Ottawa, ON, Canada

Paolo M. Ossi, NEMAS - WIBIDI Lab, Politecnico di Milano, Milano, Italy

Kaoru Yamanouchi, Department of Chemistry, The University of Tokyo, Tokyo, Japan

Topics in Applied Physics is a well-established series of review books, each of which presents a comprehensive survey of a selected topic within the domain of applied physics. Since 1973 it has served a broad readership across academia and industry, providing both newcomers and seasoned scholars easy but comprehensive access to the state of the art of a number of diverse research topics.

Edited and written by leading international scientists, each volume contains high-quality review contributions, extending from an introduction to the subject right up to the frontiers of contemporary research.

Topics in Applied Physics strives to provide its readership with a diverse and interdisciplinary collection of some of the most current topics across the full spectrum of applied physics research, including but not limited to:

- Quantum computation and information
- Photonics, optoelectronics and device physics
- Nanoscale science and technology
- Ultrafast physics
- Microscopy and advanced imaging
- Biomaterials and biophysics
- Liquids and soft matter
- Materials for energy
- Geophysics
- Computational physics and numerical methods
- Interdisciplinary physics and engineering

We welcome any suggestions for topics coming from the community of applied physicists, no matter what the field, and encourage prospective book editors to approach us with ideas. Potential authors who wish to submit a book proposal should contact Zach Evenson, Publishing Editor:

zachary.evenson@springer.com

Topics in Applied Physics is included in Web of Science (2020 Impact Factor: 0.643), and is indexed by Scopus.

More information about this series at <https://link.springer.com/bookseries/560>

Noé Jiménez · Olga Umnova · Jean-Philippe Groby
Editors

Acoustic Waves in Periodic Structures, Metamaterials, and Porous Media

From Fundamentals to Industrial Applications

Editors

Noé Jiménez
I3M
Universitat Politècnica de València
Valencia, Spain

Olga Umnova
Acoustics Research Centre
University of Salford
Salford, UK

Jean-Philippe Groby
Laboratoire d'Acoustique de l'Université
du Mans (LAUM)
Institut d'Acoustique - Graduate School (IA
- GS)
Le Mans, France

ISSN 0303-4216

ISSN 1437-0859 (electronic)

Topics in Applied Physics

ISBN 978-3-030-84299-4

ISBN 978-3-030-84300-7 (eBook)

<https://doi.org/10.1007/978-3-030-84300-7>

© The Editor(s) (if applicable) and The Author(s), under exclusive license to Springer Nature Switzerland AG 2021, corrected publication 2022

This work is subject to copyright. All rights are solely and exclusively licensed by the Publisher, whether the whole or part of the material is concerned, specifically the rights of translation, reprinting, reuse of illustrations, recitation, broadcasting, reproduction on microfilms or in any other physical way, and transmission or information storage and retrieval, electronic adaptation, computer software, or by similar or dissimilar methodology now known or hereafter developed.

The use of general descriptive names, registered names, trademarks, service marks, etc. in this publication does not imply, even in the absence of a specific statement, that such names are exempt from the relevant protective laws and regulations and therefore free for general use.

The publisher, the authors and the editors are safe to assume that the advice and information in this book are believed to be true and accurate at the date of publication. Neither the publisher nor the authors or the editors give a warranty, expressed or implied, with respect to the material contained herein or for any errors or omissions that may have been made. The publisher remains neutral with regard to jurisdictional claims in published maps and institutional affiliations.

This Springer imprint is published by the registered company Springer Nature Switzerland AG
The registered company address is: Gewerbestrasse 11, 6330 Cham, Switzerland

To our families

Preface

Noise, especially at low frequencies, is a major environmental problem across Europe. Increasingly more information is becoming available about the health impacts of noise. The latest publication of the World Health Organization (WHO) and the Joint Research Center of the European Commission shows that traffic-related noise may account for over 1 million healthy years of life lost annually in the European Union (EU) Member States and other Western European countries. In addition, the Guidelines for EU Noise acknowledge effects of environmental noise, including annoyance, as a serious health problem. According to the European Environment Agency, more than 30% of the EU population may be exposed to excessive noise levels causing annoyance, fatigue, and sleep disturbance.

Urbanization, growing demand for motorized transport, and inefficient urban planning are the main driving forces for environmental noise exposure. There is a pressing need for lighter, thinner, and more efficient structures for the absorption of low frequency sound. Until now, porous materials have been the common choice for noise and vibration control due to their ability to dissipate vibro-acoustic energy through thermal and viscous losses. However, bulky and heavy porous material treatments are required to absorb low frequency sound and mitigate low frequency elastic energy. In addition, in many engineered systems (such as aircraft) the multifunctionality of the noise reducing components, which need to carry mechanical loads and provide thermal or electromagnetic insulation, is essential. This cannot be achieved using conventional porous materials.

For many years the development of noise reducing treatments has been the subject purely of acoustics research. However, recent scientific advances provide a unique and timely opportunity to bring about significant improvements in the design of noise treatments. Phononic and sonic crystals, acoustic metamaterials, and metasurfaces can revolutionize noise and vibration control and in many cases replace traditional porous material. The major breakthroughs are expected in the areas where the traditional acoustics overlaps with new branches of physics and mechanics. Moreover, it is expected that not just attenuation, but also manipulation of sound and vibration by compact devices and structures will be an important next step in addressing this issue. It is therefore necessary to unite the efforts of all the scientific

communities involved. The first action is to provide a common theoretical background to the different communities, researchers and engineers, working on acoustic metamaterials, metasurfaces, and sonic crystals as well as conventional acoustic materials.

The Training School *Sound waves in metamaterials and porous media* has been organized by the DENORMS COST Action (CA15125) in order to facilitate this. The Trainers decided to write the present book with the aim of providing the theoretical background on acoustic materials for the researchers from different communities. It is thus organized into three parts. Each part comprises a theoretical part illustrated by examples. The Part I (Chaps. 1–4) focuses on the wave propagation in periodic media and describes the commonly used modeling techniques such as Plane Wave Expansion, Multiple Scattering theory, and Transfer Matrix Method. The illustrating example considers their application to the analysis of the sonic crystal performance. The subject of the Part II (Chaps. 5–8) is the acoustic wave propagation in metamaterial and porous absorbers with viscothermal losses. The recent advances in the design of acoustic metamaterials are first reviewed. The acoustic wave propagation in viscothermal effective fluids, i.e., porous media, and the extension of this theory to non-local models for fluid saturated metamaterials are then considered. Numerical methods, relevant to this problem, are described in detail. Finally, the Part III (Chaps. 9–12) offers a review of industrial applications targeted at building, automotive, and aeronautic industry. This part is thought as a white book for these three industries.

In this book, we have tried to cover theoretical background of the subject, related solution methods, and applications, in order to equip the reader with the skills essential for a successful researcher. The Editors would like to thank the participants, both the Trainers and the Trainees, of the Training School *Sound waves in metamaterials and porous media* and the authors of each chapter. This book is the result of a huge collective effort over years and we hope it will be useful for the current and future generations of researchers in the field of acoustic materials.

Le Mans, France
Salford, UK
Valencia, Spain
November 2019

Jean-Philippe Groby
Olga Umnova
Noé Jiménez

Contents

Part I Wave Propagation in Periodic and Structured Media

1	Periodic Structures, Irreducible Brillouin Zone, Dispersion Relations and the Plane Wave Expansion Method	3
	Jérôme O. Vasseur	
1.1	Preamble	3
1.2	One-Dimensional Atomic Chains	4
1.2.1	One Dimensional Atomic Chain With One Atom by Unit Cell	4
1.2.2	One Dimensional Atomic Chain With Two Atoms Per Unit Cell	6
1.3	Elements of Crystallography	8
1.3.1	Bravais Lattice, Primitive Vectors, Wigner-Seitz Cell	8
1.3.2	Reciprocal Lattice, Irreducible Brillouin Zone	9
1.3.3	Examples	11
1.4	The Plane Wave Expansion Method	15
1.4.1	Plane Wave Expansion Method for Bulk Phononic Crystals	15
1.4.2	Limitations of the PWE Method	28
1.4.3	Modified PWE Method for Complex Band Structures	34
1.4.4	PWE Method for 2D Phononic Crystal Plates	37
1.5	Conclusions	40
	References	41
2	Introduction to Multiple Scattering Theory for Scalar Waves	43
	Dani Torrent	
2.1	Introduction	43
2.2	Multiple Scattering of Acoustic Waves	45
2.2.1	Incident Fields	46
2.2.2	T-Matrix of a Fluid Cylinder	48

2.2.3	Multiple Scattering	50
2.3	Multiple Scattering of Flexural Waves	53
2.3.1	Effective T-Matrix	56
2.3.2	Scattering by a Cluster of Mass-Spring Resonators	57
2.4	Numerical Examples	60
	References	63
3	Sound Wave Propagation in Sonic Crystals	65
	Vicent Romero-García	
3.1	Introduction: Origins of Sonic Crystals	65
3.2	The Physical Origin of Bandgaps	67
3.2.1	Transfer Matrix Method	68
3.2.2	Discussion	68
3.3	Dispersion Relation of Sonic Crystals	71
3.3.1	Plane Wave Expansion	71
3.3.2	Extended Plane Wave Expansion	73
3.3.3	Structure Factor	74
3.3.4	Supercell Approximation	76
3.4	Multiple Scattering Theory	77
3.4.1	Cylindrical Waves	77
3.4.2	Boundary Conditions	82
3.5	Research on Sonic Crystals	85
3.5.1	Long Wavelength Regime	86
3.5.2	Diffraction Regime	88
3.6	Technological Application: Sonic Crystal Acoustic Barrier	93
3.6.1	Design Process	94
3.6.2	Acoustic Standardization	96
3.6.3	Wind Tunnel Analysis: Structural Load	96
	References	97
4	The Transfer Matrix Method in Acoustics	103
	Noé Jiménez, Jean-Philippe Groby, and Vicent Romero-García	
4.1	Introduction	103
4.2	The Transfer Matrix Method	104
4.2.1	Total Transfer Matrix	106
4.2.2	Effective Parameters	108
4.2.3	The Scattering Matrix	109
4.2.4	Reflection, Transmission and Absorption Coefficients	110
4.3	Review of the Usual Transfer Matrices	115
4.3.1	Particle Velocity Verses Flow Formulation	115
4.3.2	Fluid Layers: Particle Velocity Formulation	116
4.3.3	Ducts: Flow Formulation	117
4.3.4	Porous Media Layers	121
4.3.5	Locally Resonant Elements	126
4.3.6	Side Resonating Ducts	128

4.3.7	Helmholtz Resonators	130
4.3.8	Rigid Micro-perforated Plates	132
4.3.9	Elastic Plates	133
4.3.10	Membranes	136
4.3.11	Infinite Elastic Vibrating Wall	138
4.4	Examples of Application	140
4.4.1	Absorption of Multilayered Porous Structure	140
4.4.2	Noise Transmission Through a Double Wall	144
4.4.3	Phononic Crystals	151
4.4.4	Metamaterial Modelling Using TMM	156
4.5	Conclusions	160
4.6	Appendix—End Corrections	160
4.6.1	Change of Section in a Waveguide	161
4.6.2	Side Branch	161
4.6.3	Periodic Array of Slits	161
	References	162

Part II Wave Propagation in Absorbing Metamaterials and Porous Media

5	Acoustic Metamaterial Absorbers	167
	Jean-Philippe Groby, Noé Jiménez, and Vicent Romero-García	
5.1	Introduction	168
5.1.1	The Scattering Matrix	169
5.1.2	Complex Frequency Plane Analysis	171
5.1.3	Perfect Absorption and Critical Coupling	171
5.2	Reflection Problems	172
5.2.1	Rigidly-Backed Porous Materials	173
5.2.2	Metaporous Absorbers	175
5.2.3	Metamaterials Based on Resonant Air Cavities	178
5.2.4	Metamaterials Based in Resonant Elastic Plates and Membranes	181
5.3	Transmission Problems	183
5.3.1	Absorption and Fabry–Pérot Modes: Limits of Absorption by Single Resonators in the Transmission Problem	184
5.3.2	Monopolar and Dipolar Resonances	186
5.3.3	Overlapping of Resonances in Porous Layers	188
5.3.4	Accumulation of Resonances Due to Dispersion	190
5.3.5	Symmetry Breaking Materials	193
5.3.6	Combinations of Monopolar and Dipolar Resonances	196
5.4	Summary and Conclusions	199
	References	201

6	Acoustic Wave Propagation in Viscothermal Fluids	205
	Denis Lafarge	
6.1	Introduction	205
6.2	Molecular Constitution of Fluids	207
6.3	Wave Propagation in a Viscothermal Fluid: <i>Use of Near-Equilibrium Thermodynamics Because of Scale Separation</i>	210
6.4	Governing Navier-Stokes-Fourier Equations for Small Amplitude Wave Propagation	212
6.5	Equilibrium Thermodynamics: <i>Brief Recap on Trivariate Fluids</i>	214
6.6	Derivation of the Equations of Motion	217
6.6.1	Conservation Laws and Equation of State	218
6.6.2	Constitutive Laws: Stokes and Fourier	221
6.6.3	Inherent Thermodynamic Simplifications in Navier-Stokes-Fourier's Framework	225
6.7	The Different Normal Modes at Fixed Real Wavevector	226
6.8	Some Explicit Calculations for the Longitudinal Modes	228
6.9	General Representation of the Fields in Harmonic Regime Without Source	231
6.10	Revisiting the Longitudinal Acoustic Equations Using an Electromagnetic Analogy	233
6.11	Macroscopic Electromagnetics	234
6.11.1	Nonlocal Maxwellian Pattern of the Macroscopic Equations	234
6.11.2	Passage from Microscopics to Macroscopics	237
6.11.3	Ambiguities and a Suggested Way to Resolve Them	240
6.11.4	Ambiguities and the Customary Way	242
6.11.5	Discussion of Our Proposal	243
6.12	Nonlocal Maxwellian Pattern of Longitudinal Acoustics	244
6.12.1	Electromagnetic Analogy	245
6.12.2	Acoustic Maxwell Fields	248
6.12.3	Acoustic Nonlocal Operators	251
6.12.4	Summary: Action-Response Problem to Determine the Acoustic Kernels $\rho(\omega, \mathbf{k})$ and $\chi^{-1}(\omega, \mathbf{k})$	256
6.12.5	Acoustics Translation of the Customary Viewpoint	257
	Appendix: Electromagnetic-Acoustic Analogy	259
	References	271
7	Nonlocal Dynamic Homogenization of Fluid-Saturated Metamaterials	273
	Denis Lafarge	
7.1	Sound Propagation in Fluid-Saturated Rigid-Framed Porous Media	273

7.2	Statement of the Problem	275
7.3	The Operations of Macroscopic Averaging	278
7.3.1	The Well-Defined Case of Stationary-Random Media	279
7.3.2	The Ambiguous Case of Periodic Media	288
7.4	Macroscopic Equations and Definition of the Acoustic H -Field from Electromagnetic Analogy	295
7.4.1	Unbounded Fluid (Longitudinal Motions)	296
7.4.2	Macroscopic Electromagnetics	297
7.4.3	Macroscopic Acoustics (Fluid-Saturated Rigid-Framed Porous Medium)	298
7.5	Macroscopic Equations: Other Points of View	300
7.5.1	Macroscopic Electromagnetics—Customary Point of View	300
7.5.2	Acoustics Translation of the Customary Point of View in Electromagnetics	301
7.5.3	Acoustics Formulation in Terms of Volume-Averaged Pressure	301
7.6	Derivation of the Macroscopic Equations by a Micro-Macro Passage	303
7.7	Action-Response Problem to Determine the Nonlocal Dynamic Operators from Microstructure	307
7.8	Other Points of View	311
7.8.1	Acoustics Translation of the Customary Point of View in Electromagnetics	311
7.8.2	Acoustics Formulation in Terms of Volume-Averaged Pressure	313
7.9	Characteristic Wavenumbers and Impedances	314
7.10	Conclusions	315
	Appendix: Local Dynamic Homogenization of Rigid-Framed Fluid-Saturated Porous Materials	316
	References	330
8	Numerical Methods for Modelling and Simulation of Porous Materials	333
	Peter Goransson and Olivier Dazel	
8.1	Introduction	333
8.2	Biot's Equations	335
8.2.1	Constitutive Laws	336
8.2.2	Momentum Equations	337
8.3	Weak Forms	339
8.3.1	PEM1 Weak Formulation	339
8.3.2	PEM2 Weak Formulation	339
8.3.3	Elastic Solid	340
8.3.4	Air	341

8.4 Discrete Linear System 341

8.4.1 Elementary Matrices 341

8.4.2 Discretisation of the Weak Forms in One Element 342

8.4.3 Assembly 344

8.5 Coupling Between Domains 345

8.5.1 Coupling with an Air Domain 345

8.5.2 Coupling with an Elastic Solid 347

8.5.3 Coupling Through a Thin Airgap Interface 348

8.5.4 Coupling with Bloch Waves 350

8.6 Application Examples 352

8.6.1 Convergence Aspects 353

8.6.2 FE Cases in 1D 354

8.6.3 Simulation of a Metaporous Material 359

8.6.4 3D Anisotropic Modelling 362

Appendix - Periodic Boundary Conditions 364

References 365

Part III Industrial Applications of Porous Media and Acoustic Metamaterials

9 Industrial Applications I 369

Arnaud Duval and Fabien Chevillotte

9.1 Introduction 369

9.2 Absorption Optimization 370

9.2.1 The Coupling Parameters:
Johnson-Champoux-Allard (JCA) Model 371

9.2.2 Optimizing Felts or Fibrous Materials
for Absorption 373

9.2.3 Optimizing Foam Materials for Absorption 375

9.2.4 Airflow Resistive Screens: Tunable Absorption 379

9.3 Insulation Optimization 383

9.3.1 Insulation Optimization: Fibrous Porous Material
Case 384

9.3.2 Insulation Optimization: Foam Porous Material
Case 384

9.3.3 The Standard Mass—Poroelastic Spring Insulator 384

9.3.4 The Hybrid Stiff Insulator Concept 385

9.4 Damping Optimization 386

9.4.1 Damping Optimization: Poroelastic Material Itself 386

9.4.2 Damping Optimization: Poroelastic Material
Boundary Conditions 387

9.5 Conclusions 388

References 388

10 Industrial Applications II	391
Fabien Chevillotte	
10.1 Introduction	391
10.2 Acoustical Applications in the Building Industry	392
10.2.1 Acoustical Correction	392
10.2.2 Air-Borne Insulation	393
10.2.3 Solid-Borne Insulation (Impact Noise)	400
10.2.4 Ceilings	401
10.3 New Trends in Building Acoustics	402
10.3.1 Thin and Aesthetic Absorbers	402
10.3.2 Low Frequency Performances and Non-conventional Phenomena	402
10.3.3 Rolling Noise	404
10.4 Conclusions	405
References	405
11 Industrial Applications III	407
Arnaud Duval	
11.1 Introduction	407
11.2 Acoustic Package Optimization Methods in the Automotive Industry	408
11.2.1 Automotive Vehicle Main Noise Sources and Airborne Transfer Paths	408
11.2.2 Multilayer Noise Treatments Properties	412
11.3 Fast Broadband Highly Curved Insertion Loss Simulation of Automotive Trims	418
11.3.1 Trim Modelling Curvature Issue	418
11.3.2 Cylindrical Transfer Matrix Method: A Spectral Approach	419
11.3.3 Curvature Radius Influence on Trim Insertion Loss Slopes	421
11.3.4 Trim Thickness Influence on Curved Insertion Loss Breathing Frequencies	421
11.3.5 Multi-thickness Simplified 3D Dash Insulator Broadband Insertion Loss Simulation	423
11.3.6 Summary of Curved Insertion Loss Simulations	426
11.4 Conclusions	426
References	427
12 Industrial Applications IV	429
Israel Pereira, Sideto Futatsugi, and Maria L. V. Rodrigues	
12.1 Introduction	429
12.2 Description of Noise Sources	430
12.2.1 Engine Sources	430
12.2.2 Turbulent Boundary Layer (TBL)	431
12.2.3 Systems	432

12.3	The Use of Porous Materials	433
12.4	Aeronautic Requirements	435
12.5	New Developments	436
12.6	Case Study	437
	References	440
	Correction to: Acoustic Wave Propagation in Viscothermal Fluids	C1
	Denis Lafarge	
	Index	441

Contributors

Fabien Chevillotte MATELYS - Research Lab., Bât. B, 7 Rue des Maraîchers, Vaulx-En-Velin, France

Olivier Dazel University of Le Mans, UMR CNRS 6613, Le Mans, France

Arnaud Duval Trèves Products, Services & Innovation, 2-4 rue Emile Arquès, Reims, France;

TREVES Product, Services & Innovation, 2–4 rue Emile Arquès, Reims, France

Sideto Futatsugi Embraer S.A, Av. Brigadeiro Faria Lima, São José dos Campos, Brazil

Peter Goransson KTH Royal Institute of Technology, Stockholm, Sweden

Jean-Philippe Groby Laboratoire d'Acoustique de l'Université du Mans, UMR CNRS 6613, Le Mans Université, Le Mans, France

Noé Jiménez Instituto de Instrumentación para Imagen Molecular, Universitat Politècnica de València, CSIC, Camino de Vera S/N, València, Spain

Denis Lafarge Laboratoire d'Acoustique de l'Université du Mans, UMR CNRS 6613, Le Mans Université, Le Mans, France

Israel Pereira Embraer S.A, Av. Brigadeiro Faria Lima, São José dos Campos, Brazil

Maria L. V. Rodrigues Embraer R&D Portugal, Parque da Indústria Aeronáutica de Évora, Lote A-I, Herdade do Pinheiro e Casa Branca, Évora, Portugal

Vicent Romero-García Laboratoire d'Acoustique de l'Université du Mans, UMR CNRS 6613, Le Mans Université, Le Mans, France

Dani Torrent Grup de Recerca d'òptica (GROC), Institut de Noves Tecnologies de la Imatge (INIT), Universitat Jaume I, Castelló, Spain

Jérôme O. Vasseur Institute of Electronic, Microelectronic and Nanotechnology, UMR CNRS 8520, Université de Lille, Villeneuve-d'Ascq, France

Part I
Wave Propagation in Periodic and
Structured Media

Chapter 1

Periodic Structures, Irreducible Brillouin Zone, Dispersion Relations and the Plane Wave Expansion Method



Jérôme O. Vasseur

Abstract The Plane Wave Expansion (PWE) method allows the calculation of dispersion curves, i.e., the relation linking the frequency to the wave number for any propagating mode of periodic structures made of elastic materials such as phononic crystals. The method is relatively easy to implement numerically but presents some limitations. After recalling some fundamental aspects of crystallography that are necessary to the study of periodic structures, the PWE method described in detail for the case of bulk phononic crystals, i.e., structures of infinite extent, and its advantages and drawbacks are discussed. It is also shown that the method can be used for calculating the band structure of phononic crystals of finite thickness and for analysing the evanescent waves within the phononic band gaps.

1.1 Preamble

Propagation of elastic waves in composite materials exhibiting a periodic structure constitutes a very old topic in physics. One can mention the work, among others, of Lord Rayleigh in 1887 where has been demonstrated the existence of band gaps in periodically stratified media [1]. However since the beginning of the 1990s and the pioneering works of Sigalas et al. [2] and Kushwaha et al. [3] on phononic crystals, this topic received a renewed interest. These artificial material composites whose physical characteristics (density, elastic moduli, ...) are periodic functions of the position have been proven to exhibit very peculiar propagation properties such as frequency band gaps, negative refraction or self-collimation phenomena [4]. Studies of the propagation of elastic waves in periodic structures necessitate using theoretical tools that were initially developed in the frame of solid state physics such as the unit cell, the direct lattice, the reciprocal lattice, the irreducible Brillouin zone or dispersion relations. Moreover, these studies also require solving, with a high level

J. O. Vasseur (✉)

Institute of Electronic, Microelectronic and Nanotechnology, UMR CNRS 8520, Université de Lille, Villeneuve-d'Ascq, France
e-mail: jerome.vasseur@univ-lille.fr

of accuracy, the equations of elastic waves propagation. Different theoretical tools were proposed for this. One can mention the Plane Wave Expansion (PWE) method, the Finite Difference Time Domain (FDTD) method, the Multiple Scattering (MS) method, the Finite Element (FE) method, and many others [4].

With the aim of introducing in a pedagogical way most of the solid state physics concepts listed above, very simple periodic structures such as one dimensional infinite atomic chains are considered first. In the second part of this Chapter, we recall in a more formal way, the elements of crystallography that are necessary for the study of periodic structures. The third part of the Chapter focuses on the PWE method. Basic principles of the method are first presented and its application to two-dimensional periodic structures is reported with many details. Limitations of the PWE method are discussed. Finally, it is also shown that the method can be used for calculating the band structure of phononic crystals of finite thickness and for analysing the evanescence of waves inside the phononic band gaps.

1.2 One-Dimensional Atomic Chains

1.2.1 One Dimensional Atomic Chain With One Atom by Unit Cell

We consider first a very simple periodic structure, namely an infinite one-dimensional linear chain of identical atoms with mass m , connected by springs with constant stiffness β and oriented along the x direction. The equilibrium position of atom n is $x_{n,eq} = na$, where a is the distance between two adjacent atoms in equilibrium. Atoms are assumed free to move slightly around their respective equilibrium position and their position, at any time t , is given as $x_n(t) = na + u_n(t)$ with $|u_n(t)| \ll |x_n(t)|$ and $u_n = x_n - x_{n,eq}$ is the displacement of the n^{th} atom from the equilibrium position. In that case, the unit cell, shown in Fig. 1.1, that can be repeated along direction x with periodicity a , contains only one atom and the lattice spacing a defines the periodicity of the chain along the x axis. Newton's second law applied to atom n considering interaction between nearest neighbours leads to

$$m \frac{\partial^2 u_n}{\partial t^2} = -\beta (u_n - u_{n-1}) + \beta (u_{n+1} - u_n) = \beta (u_{n+1} + u_{n-1} - 2u_n). \quad (1.1)$$

Seeking solutions of Eq. (1.1) in the form of sinusoidal propagating waves of amplitude U_0 such as $u_n(t) = U_0 e^{i(kna - \omega t)}$ where k is the wave number and ω the circular frequency, Eq. (1.1) becomes

$$-m\omega^2 = \beta (e^{ika} + e^{-ika} - 2) = 2\beta (\cos(ka) - 1) = -4\beta \sin^2\left(\frac{ka}{2}\right). \quad (1.2)$$

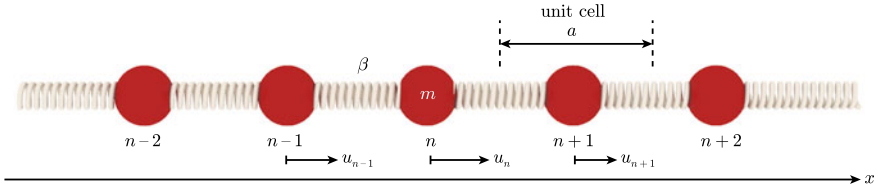


Fig. 1.1 Schematic illustration of the infinite atomic chain made of identical atoms of mass m with a lattice parameter a . β is the stiffness of the spring linking atoms

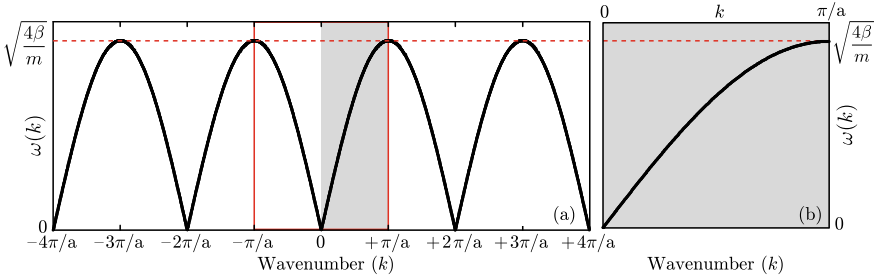


Fig. 1.2 **a** Dispersion relation of the infinite atomic chain made of identical atoms. The red and shaded boxes represent the first Brillouin zone and the irreducible Brillouin zone, respectively; **b** Dispersion relation plotted in the irreducible Brillouin zone

One deduces from Eq. (1.2), the dispersion relation of the atomic chain, i.e., the relation linking the circular frequency ω to the wave number k in the form

$$\omega(k) = \sqrt{\frac{4\beta}{m}} \left| \sin\left(\frac{ka}{2}\right) \right|. \quad (1.3)$$

Figure 1.2a shows the dispersion relation $\omega(k)$. Note that $|\sin(ka/2)|$ is a π -periodic function,

$$\left| \sin\left(\frac{ka}{2}\right) \right| = \left| \sin\left(\frac{ka}{2} + \pi\right) \right| = \left| \sin\left(\frac{a}{2} \left[k + \frac{2\pi}{a} \right] \right) \right|. \quad (1.4)$$

Then, $\omega(k)$ is a periodic function of k with periodicity $G = 2\pi/a$ and $\omega(k + nG) = \omega(k)$ where n is an integer. One deduces that a propagation mode of wave number k and a mode with wave number $(k + G)$ are exactly the same modes. The periodicity $G = 2\pi/a$ in the wave number space is associated with the *reciprocal lattice* of the chain while the lattice parameter a characterizes its *direct lattice*.

Due to the periodicity of the dispersion relation in the reciprocal space, the useful information concerning the vibration modes that can propagate in the chain, is contained in the waves with wave numbers lying between the limits $-\pi/a$ and $+\pi/a$. This range of wave numbers centred at $k = 0$ is named the *first Brillouin zone* of the reciprocal lattice. Therefore, the dispersion relation is also symmetric with respect

of the plane $k = 0$, and one may restrict the study to the *irreducible Brillouin zone*, i.e., the domain of wave numbers ranging from 0 to $+\pi/a$, as shown in Fig. 1.2b.

1.2.2 One Dimensional Atomic Chain With Two Atoms Per Unit Cell

We can now turn to a little bit more complicated structure: an infinite one-dimensional linear chain with two atoms of different masses in the unit cell, as shown in Fig. 1.3. The lattice parameter is $2a$ and all the springs are supposed to have the same stiffness β . Atoms of mass m_1 and m_2 are named *even* and *odd* atoms and are labelled with integers $2n$ and $2n + 1$ respectively.

With the same assumptions as that of Sect. 1.2.1, we can write the equations of motion for *even* and *odd* atoms in the form

$$\begin{cases} m_1 \frac{\partial^2 u_{2n}}{\partial t^2} = -\beta (u_{2n} - u_{2n-1}) + \beta (u_{2n+1} - u_{2n}) \\ \quad = \beta (u_{2n+1} + u_{2n-1} - 2u_{2n}), \\ m_2 \frac{\partial^2 u_{2n+1}}{\partial t^2} = -\beta (u_{2n+1} - u_{2n}) + \beta (u_{2n+2} - u_{2n+1}) \\ \quad = \beta (u_{2n+2} + u_{2n} - 2u_{2n+1}). \end{cases} \quad (1.5)$$

Seeking solutions of Eq. (1.5) in the form

$$\begin{cases} u_{2n}(t) = A e^{i(k(2n)a - \omega t)}, \\ u_{2n+1}(t) = B e^{i(k(2n+1)a - \omega t)}, \end{cases} \quad (1.6)$$

where A and B are amplitude terms, one obtains a set of two equations that can be recast in the following matrix form

$$\begin{bmatrix} (2\beta - m_1\omega^2) & -2\beta \cos(ka) \\ 2\beta \cos(ka) & -(2\beta - m_2\omega^2) \end{bmatrix} \begin{bmatrix} A \\ B \end{bmatrix} = \begin{bmatrix} 0 \\ 0 \end{bmatrix}. \quad (1.7)$$

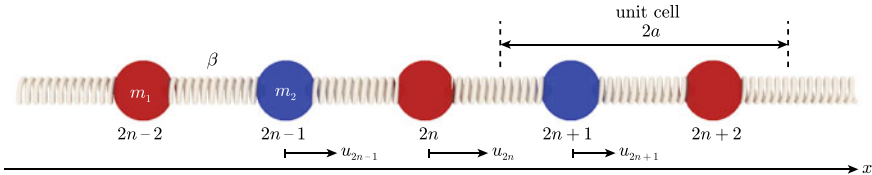


Fig. 1.3 Schematic illustration of the infinite atomic chain made of two atoms of masses m_1 and m_2 in the unit cell with a lattice parameter $2a$. β is the stiffness of the spring linking atoms

Equations (1.7) admit non-trivial solutions if the determinant of the matrix vanishes. This leads to

$$\omega^4 - 2\beta \left(\frac{m_1 + m_2}{m_1 m_2} \right) + \frac{4\beta^2 \sin^2(ka)}{m_1 m_2} = 0, \quad (1.8)$$

and one deduces

$$\omega(k) = \sqrt{\beta \frac{m_1 + m_2}{m_1 m_2} \left(1 \pm \sqrt{1 - 4 \frac{m_1 m_2 \sin^2(ka)}{(m_1 + m_2)^2}} \right)}. \quad (1.9)$$

Consequently, Eq. (1.8) admits two real solutions $\omega_-(k)$ and $\omega_+(k)$ that are periodic in wave number, k , with a period of $+\pi/a$ and the first Brillouin zone corresponds to the wave numbers varying between $-\pi/2a$ and $+\pi/2a$. One notes that because the unit cell in the direct lattice of the chain is two times larger than that of the monoatomic chain, the first Brillouin zone is two times smaller. Figure 1.4 shows the dispersion relations plotted in the irreducible Brillouin zone (k between 0 and $+\pi/2a$) as a function of the ratio m_2/m_1 greater than or equal to 1. One observes that for $m_2 = m_1$, the dispersion relation of the infinite monoatomic chain is recovered but the band is folded in a smaller irreducible Brillouin zone. Moreover, for increasing mass ratio, a band gap appears at the edge of the irreducible Brillouin zone and higher is the mass ratio, the larger is the band gap.

In this Section, considering very simple one dimensional periodic structures, we have introduced the notions that are of fundamental importance in the study of periodic structures namely the unit cell, the direct and reciprocal lattices and the irreducible Brillouin zone. We will see in Sect. 1.3.1 of this Chapter, how these concepts can be generalized of much more complicated periodic structures such as the phononic crystals.

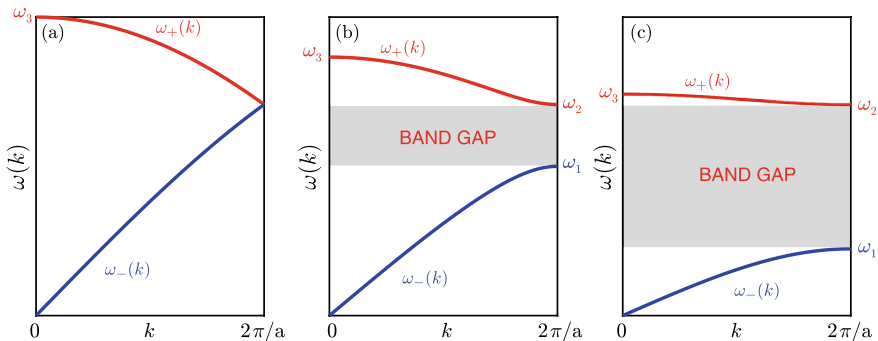


Fig. 1.4 Dispersion relations of the infinite atomic chain made of two atoms of masses m_1 and m_2 in the unit cell with a lattice parameter $2a$ plotted in the irreducible Brillouin zone for **a** $m_2 = m_1$, **b** $m_2 = 2m_1$, **c** $m_2 = 10m_1$. Circular frequencies ω_1 , ω_2 and ω_3 are equal to $\sqrt{2\beta/m_2}$, $\sqrt{2\beta/m_1}$, $\sqrt{2\beta(m_1 + m_2)/m_1 m_2}$, respectively

1.3 Elements of Crystallography

In this Section, we recall the elements of crystallography that are necessary for the study of periodic structures. We limit ourselves to some simple structures. Complete reports on solid state physics are available in text books such as Refs. [5, 6]. These references are strongly recommended to the reader of the present Chapter.

1.3.1 Bravais Lattice, Primitive Vectors, Wigner-Seitz Cell

In solid state physics, solids possessing a crystalline structure are periodic arrays of atoms that are modelled by a combination of a basis and a Bravais lattice. In Ref. [6], a Bravais lattice is defined as: *an infinite array of discrete points with an arrangement and orientation that appear exactly the same, from whichever of the points the array is viewed (all the points have the same environment).*

In three dimensions (3D), there exist a total of fourteen different Bravais lattices [5, 6], five in 2D and one in 1D. The symmetry of any physical crystal is described by one of the Bravais lattices plus a basis. The basis consists of identical units, usually made by group of atoms, which are attached to every point of the underlying Bravais lattice. A crystal, whose basis consists of a single atom or ion, is said to have a monatomic Bravais lattice.

In 3D, from the mathematical point of view, a Bravais lattice is defined as a collection of points with position vectors \vec{R} of the form $\vec{R} = \ell\vec{a}_1 + m\vec{a}_2 + n\vec{a}_3$ where \vec{a}_1 , \vec{a}_2 and \vec{a}_3 are three vectors (named *the primitive vectors of the Bravais lattice*) not in the same plane and ℓ , m and n are three integers. For the sake of simplicity, the notion of Bravais lattice is illustrated in 2D on Fig. 1.5. In this figure, one observes that from a point chosen at the origin of the array, any other point can be obtained by a translation equals to a linear combination of the primitive vectors. Moreover for any given Bravais lattice, the set of primitive vectors is not unique, as shown in Fig. 1.5. Characterization of an array of points requires also to define a volume of space that contains precisely one lattice point and can be translated through all the vectors of a Bravais lattice to fill all the space without overlapping itself or leaving voids. This space is named a primitive cell and is depicted also in Fig. 1.5. There is no unique way of choosing a primitive cell but the most common choice, however, is the Wigner-Seitz cell, which has the full symmetry of the underlying Bravais lattice. The Wigner-Seitz cell about a lattice point also has a property of being closer to that point than to any other lattice point. It can be constructed by drawing lines connecting a given point to nearby lying points, bisecting each line with a plane and taking the smallest polyhedron bounded by these planes. The Bravais lattice, which is defined in real space, is sometimes referred to as a direct lattice.

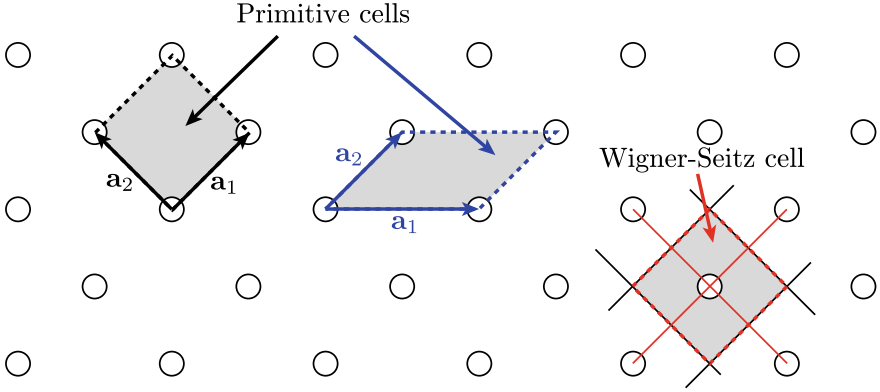


Fig. 1.5 A 2D Bravais lattice. Two possible choices of the primitive vectors \vec{a}_1 and \vec{a}_2 are indicated. Black and blue parallelograms represent the primitive unit cells associated with each set of primitive vectors. Red parallelogram is the Wigner-Seitz cell of the Bravais lattice. It has been constructed by drawing red lines connecting a given point to nearby lying points, drawing black lines bisecting each red line and considering the area bounded by red dashed lines

1.3.2 Reciprocal Lattice, Irreducible Brillouin Zone

With the direct lattice being defined in the real space, there exists a dual space named the reciprocal lattice. This concept is very important when studying wave propagation, diffraction and other wave phenomena in crystals. We know that in the direct lattice, a periodic function in space $f(\vec{r})$ satisfies $f(\vec{r}) = f(\vec{r} + \vec{R})$ where $\vec{R} = \ell\vec{a}_1 + m\vec{a}_2 + n\vec{a}_3$, see Sect. 1.3.1. For example, the function $f(\vec{r})$ in phononic crystals can be the mass density or the elastic moduli. This function being R -periodic can be developed in Fourier series such as

$$f(\vec{r}) = \sum_{\vec{G}} f(\vec{G}) e^{i\vec{G} \cdot \vec{r}}, \quad (1.10)$$

where \vec{G} are named the *reciprocal lattice vectors* and $f(\vec{G})$ are the Fourier coefficients of $f(\vec{r})$. Then one can write

$$f(\vec{r} + \vec{R}) = \sum_{\vec{G}} f(\vec{G}) e^{i\vec{G} \cdot (\vec{r} + \vec{R})} = f(\vec{r}) = \sum_{\vec{G}} f(\vec{G}) e^{i\vec{G} \cdot \vec{r}}, \quad (1.11)$$

and one deduces that $e^{i\vec{G} \cdot \vec{R}} = 1$ and $\vec{G} \cdot \vec{R} = 2\pi \cdot N$ where N is an integer. Consequently, one can define the reciprocal lattice as a set of points whose positions are given by a set of vectors \vec{G} satisfying the condition

$$\vec{G} \cdot \vec{R} = 2\pi \cdot N; \quad N \in \mathbb{Z}, \quad (1.12)$$

for all \vec{R} in the Bravais lattice. Searching for a mathematical form for the \vec{G} vectors, we assume that because \vec{R} is a linear combination of the primitive vectors \vec{a}_i , $i = 1, 2, 3$, \vec{G} may be written also as a linear combination of some basis vectors \vec{b}_i , $i = 1, 2, 3$ as $\vec{G} = \ell'\vec{b}_1 + m'\vec{b}_2 + n'\vec{b}_3$ where ℓ', m', n' and the \vec{b}_i are initially undefined. Equation (1.12) leads to

$$\begin{aligned} \ell'\vec{b}_1 \cdot \vec{a}_1 + m'\vec{b}_2 \cdot \vec{a}_1 + n'\vec{b}_3 \cdot \vec{a}_1 + \\ + \ell'm\vec{b}_1 \cdot \vec{a}_2 + m'm\vec{b}_2 \cdot \vec{a}_2 + m'n\vec{b}_2 \cdot \vec{a}_3 + \\ + n'\ell\vec{b}_3 \cdot \vec{a}_1 + n'm\vec{b}_3 \cdot \vec{a}_2 + n'n\vec{b}_3 \cdot \vec{a}_3 = 2\pi N. \end{aligned} \quad (1.13)$$

One may impose the basis $\{\vec{b}_i\}$ to be orthonormal to the basis $\{\vec{a}_i\}$ and write $\vec{b}_i \cdot \vec{a}_j = 2\pi\delta_{ij}$ where δ_{ij} is the Kronecker's symbol and the multiplicative factor 2π has been introduced for simplification. Then Eq. (1.13) reduces to

$$\ell'\ell + m'm + n'n = N. \quad (1.14)$$

The left-hand side of Eq. (1.14) must be an integer as the right-hand side and consequently ℓ', m' and n' must be also integers. This implies that a reciprocal lattice of a direct lattice is also a Bravais lattice. We can now define vectors \vec{b}_i . Consider first \vec{b}_1 . Because $\vec{b}_1 \perp \vec{a}_2$ and $\vec{b}_1 \perp \vec{a}_3$, one may write $\vec{b}_1 = \lambda \cdot \vec{a}_2 \times \vec{a}_3$ where λ is a constant to be determined. Moreover, $\vec{a}_1 \cdot \vec{b}_1 = 2\pi = \lambda \vec{a}_1 \cdot (\vec{a}_2 \times \vec{a}_3)$ and one deduces $\lambda = 2\pi / [\vec{a}_1 \cdot (\vec{a}_2 \times \vec{a}_3)]$. The same can be done for vectors \vec{b}_2 and \vec{b}_3 and one obtains $\vec{b}_2 = 2\pi \vec{a}_3 \times \vec{a}_1 / [\vec{a}_2 \cdot (\vec{a}_3 \times \vec{a}_1)]$ and $\vec{b}_3 = 2\pi \vec{a}_1 \times \vec{a}_2 / [\vec{a}_3 \cdot (\vec{a}_1 \times \vec{a}_2)]$. One notes that $\vec{a}_1 \cdot (\vec{a}_2 \times \vec{a}_3) = \vec{a}_2 \cdot (\vec{a}_3 \times \vec{a}_1) = \vec{a}_3 \cdot (\vec{a}_1 \times \vec{a}_2)$ and the basis vectors of the reciprocal lattice depend on the basis vectors of the direct lattice as

$$\left\{ \begin{aligned} \vec{b}_1 &= 2\pi \frac{\vec{a}_2 \times \vec{a}_3}{\vec{a}_1 \cdot (\vec{a}_2 \times \vec{a}_3)}, \\ \vec{b}_2 &= 2\pi \frac{\vec{a}_3 \times \vec{a}_1}{\vec{a}_2 \cdot (\vec{a}_3 \times \vec{a}_1)}, \\ \vec{b}_3 &= 2\pi \frac{\vec{a}_1 \times \vec{a}_2}{\vec{a}_3 \cdot (\vec{a}_1 \times \vec{a}_2)}. \end{aligned} \right. \quad (1.15a)$$

$$\left\{ \begin{aligned} \vec{b}_2 &= 2\pi \frac{\vec{a}_3 \times \vec{a}_1}{\vec{a}_2 \cdot (\vec{a}_3 \times \vec{a}_1)}, \\ \vec{b}_3 &= 2\pi \frac{\vec{a}_1 \times \vec{a}_2}{\vec{a}_3 \cdot (\vec{a}_1 \times \vec{a}_2)}. \end{aligned} \right. \quad (1.15b)$$

$$\left\{ \begin{aligned} \vec{b}_3 &= 2\pi \frac{\vec{a}_1 \times \vec{a}_2}{\vec{a}_3 \cdot (\vec{a}_1 \times \vec{a}_2)}. \end{aligned} \right. \quad (1.15c)$$

In Eqs. (1.15), the scalar quantity $\vec{a}_1 \cdot (\vec{a}_2 \times \vec{a}_3)$ corresponds to the volume of the parallelepiped constructed from the three primitive vectors $\{\vec{a}_i\}$ of the original direct (Bravais) lattice, i.e., the volume of the unit cell [7]. Moreover one observes that the length of the reciprocal lattice vectors is proportional to the reciprocal of the length of the direct lattice vectors and this is the origin of the term *reciprocal lattice*.

As an example, Fig. 1.6 shows a simple-cubic Bravais lattice with a lattice constant a as well as its reciprocal lattice, which is also a simple-cubic one with a lattice constant $2\pi/a$, as follows from relations (1.15). Since the reciprocal lattice is a Bravais lattice, one can also find its Wigner-Seitz cell. The Wigner-Seitz cell of a reciprocal lattice is conventionally called a first Brillouin zone. Planes in reciprocal

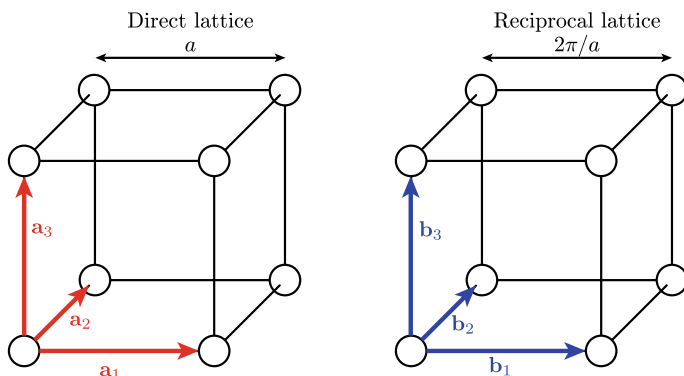


Fig. 1.6 Simple-cubic direct lattice and its reciprocal lattice. The primitive vectors of both lattices are also indicated

space, which bisect the lines joining a particular point of a reciprocal lattice with all other points, are known as Bragg planes. Therefore, the first Brillouin zone can also be defined as the set of all points in the reciprocal space that can be reached from the origin without crossing any Bragg plane. Symmetry properties may allow to reduce the dimensions of the first Brillouin zone and to define the smallest Brillouin zone also named the irreducible Brillouin zone.

In what follows we will consider, for the sake of simplicity, two examples of Bravais lattices in two dimensions, the square and the hexagonal one, and we will illustrate the concepts previously introduced.

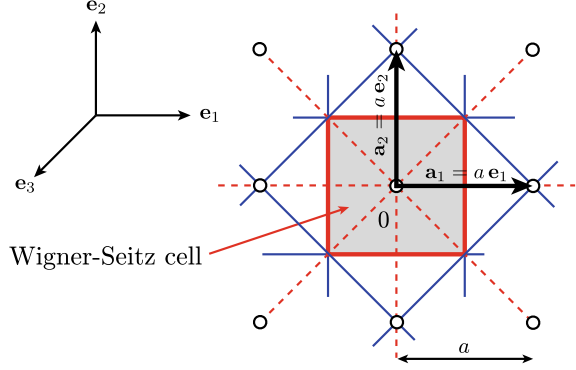
1.3.3 Examples

1.3.3.1 The Square Bravais Lattice

We first consider the case of the square Bravais lattice with lattice parameter a . The points (the “atoms”) are located at the vertices of a square as depicted in Fig. 1.7. The space is referred to an orthonormal basis $(0, \vec{e}_1, \vec{e}_2, \vec{e}_3)$ with Cartesian coordinates (x_1, x_2, x_3) and O is a point chosen as origin. The array being two-dimensional in the plane (x_1, O, x_2) , the primitive vectors of the direct lattice have components only in this plane and are $\vec{a}_1 = a\vec{e}_1$ and $\vec{a}_2 = a\vec{e}_2$ and vectors \vec{R} write $\vec{R} = a(\ell\vec{e}_1 + m\vec{e}_2)$. In Fig. 1.7, the red lines correspond to lines connecting the origin to its nearest neighbours and blue lines bisect the red dashed ones. One deduces easily from this drawing that the Wigner-Seitz cell is the grey square.

One may define now the basis vectors of the reciprocal lattice applying relations (1.15). One obtains

Fig. 1.7 The square direct lattice of lattice parameter a and its Wigner-Seitz cell



$$\left\{ \begin{array}{l} \vec{b}_1 = 2\pi \frac{a\vec{e}_2 \times \vec{e}_3}{a\vec{e}_1 \cdot (a\vec{e}_2 \times \vec{e}_3)} = \frac{2\pi}{a} \vec{e}_1, \\ \vec{b}_2 = 2\pi \frac{\vec{e}_3 \times a\vec{e}_1}{a\vec{e}_1 \cdot (a\vec{e}_2 \times \vec{e}_3)} = \frac{2\pi}{a} \vec{e}_2, \end{array} \right. \quad (1.16a)$$

$$\left\{ \begin{array}{l} \vec{b}_1 = 2\pi \frac{a\vec{e}_2 \times \vec{e}_3}{a\vec{e}_1 \cdot (a\vec{e}_2 \times \vec{e}_3)} = \frac{2\pi}{a} \vec{e}_1, \\ \vec{b}_2 = 2\pi \frac{\vec{e}_3 \times a\vec{e}_1}{a\vec{e}_1 \cdot (a\vec{e}_2 \times \vec{e}_3)} = \frac{2\pi}{a} \vec{e}_2, \end{array} \right. \quad (1.16b)$$

where \vec{e}_3 is introduced only for constructing the different cross products.

In Fig. 1.8a, the dots represent points whose positions are given by two-dimensional vectors $\vec{G} = \ell'\vec{b}_1 + m'\vec{b}_2$. One chooses point Γ as the origin of the reciprocal lattice and draws red dashed lines connecting Γ to its nearest neighbours. With the help of the blue lines bisecting the red ones, the grey square is defined as

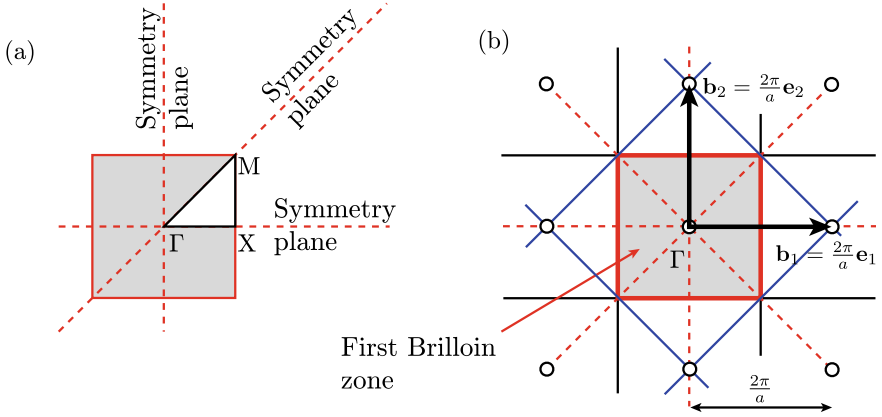


Fig. 1.8 **a** The reciprocal lattice of the square Bravais lattice and the first Brillouin zone (grey square), **b** the first Brillouin zone and the irreducible Brillouin zone (ΓXM) with $\Gamma : \frac{2\pi}{a}(0, 0)$, $X : \frac{2\pi}{a}(\frac{1}{2}, 0)$ and $M : \frac{2\pi}{a}(\frac{1}{2}, \frac{1}{2})$. Γ , X , and M are the points of highest symmetry in the irreducible Brillouin zone. In terms of wave propagation, vectors $\vec{\Gamma X}$, \vec{XM} and $\vec{\Gamma M}$ represent the principal directions of propagation

the first Brillouin zone. Due to the symmetries of the grey square, shown in Fig. 1.8b, one reduces the study to the triangle (ΓXM) where the components of point Γ in the basis (\vec{e}_1, \vec{e}_2) are $\frac{2\pi}{a}(0, 0)$. Because $\vec{\Gamma X} = \vec{b}_1/2$ and $\vec{\Gamma M} = (\vec{b}_1 + \vec{b}_2)/2$, the components of points X and M are $(\frac{2\pi}{a})(\frac{1}{2}, 0)$ and $\frac{2\pi}{a}(\frac{1}{2}, \frac{1}{2})$, respectively. The triangle (ΓXM) is the irreducible Brillouin zone of the square Bravais lattice.

When considering propagation of waves in two-dimensional phononic crystals, any wave vector \vec{k} (which belongs to the reciprocal space), can be written as $\vec{k} = \vec{G} + \vec{K}_{\text{IBZ}}$ where \vec{K}_{IBZ} belongs to the irreducible Brillouin zone. Consequently study of the propagation of waves can be limited to waves with wave vectors belonging to the irreducible Brillouin zone (see Sect. 1.2).

1.3.3.2 The Hexagonal Bravais Lattice

As depicted in Fig. 1.9, in the case of the hexagonal Bravais lattice, the “atoms” are located on the vertices and at the centre of a regular hexagon of side length a . One can construct the Wigner-Seitz cell following the same processes than that used for the square array. Around point O' the Wigner-Seitz cell has exactly the same symmetry as the direct lattice and is represented by the red hexagon. Nevertheless, due to the rather complicated geometry of the array, one may choose a simpler primitive unit cell such as the blue parallelogram constructed from the set of primitive lattice vectors

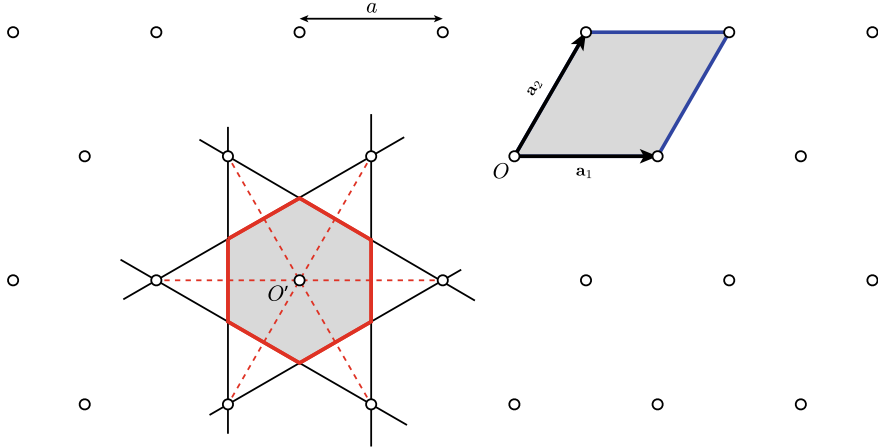


Fig. 1.9 The hexagonal direct lattice with lattice parameter a and its Wigner-Seitz cell around point O' (red hexagon). It is convenient to choose as primitive unit cell the blue parallelogram constructed from the primitive vectors $\vec{a}_1 = a\vec{e}_1$ and $\vec{a}_2 = \frac{a}{2}\vec{e}_1 + \frac{a\sqrt{3}}{2}\vec{e}_2$

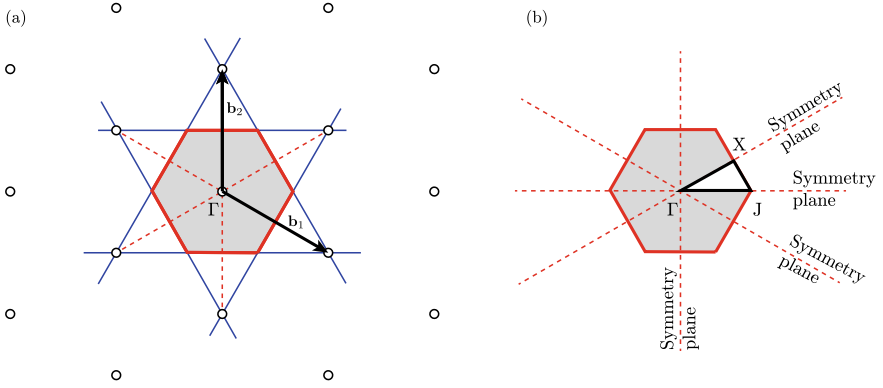


Fig. 1.10 **a** The reciprocal lattice of the hexagonal Bravais lattice and the first Brillouin zone (grey square), **b** the first Brillouin zone and the irreducible Brillouin zone (ΓJX) with $\Gamma : \frac{2\pi}{a}(0, 0)$, $J : \frac{2\pi}{a}(\frac{2}{3}, 0)$ and $X : \frac{2\pi}{a}(\frac{1}{2}, \frac{1}{2\sqrt{3}})$. Points Γ , J , and X are the points of highest symmetry in the irreducible Brillouin zone

$\{\vec{a}_1 = a\vec{e}_1, \vec{a}_2 = \frac{a}{2}\vec{e}_1 + \frac{a\sqrt{3}}{2}\vec{e}_2\}$. The basis vectors of the reciprocal lattice are then obtained using relations (1.15) as

$$\begin{cases} \vec{b}_1 = 2\pi \frac{\vec{a}_2 \times \vec{e}_3}{\vec{a}_1 \cdot (\vec{a}_2 \times \vec{e}_3)} = \frac{2\pi}{a} \left(\vec{e}_1 - \frac{1}{\sqrt{3}}\vec{e}_2 \right), & (1.17a) \end{cases}$$

$$\begin{cases} \vec{b}_2 = 2\pi \frac{\vec{e}_3 \times \vec{a}_1}{\vec{a}_1 \cdot (\vec{a}_2 \times \vec{e}_3)} = \frac{2\pi}{a} \left(\frac{2}{\sqrt{3}} \right) \vec{e}_2, & (1.17b) \end{cases}$$

and the reciprocal lattice vectors are given in the basis $(O, \vec{e}_1, \vec{e}_2)$ as $\vec{G} = \ell'\vec{b}_1 + m'\vec{b}_2 = \frac{2\pi}{a}[\ell'\vec{e}_1 + \frac{1}{\sqrt{3}}(-\ell' + 2m')\vec{e}_2]$.

The reciprocal lattice of the hexagonal array together with its first Brillouin zone are depicted in Fig. 1.10a. Due to the symmetries of the grey hexagon, shown in Fig. 1.10b, one reduces the study to the triangle (ΓJX) where the components of point Γ in the basis (\vec{e}_1, \vec{e}_2) are $\frac{2\pi}{a}(0, 0)$. Because $\vec{\Gamma X} = (\vec{b}_1 + \vec{b}_2)/2$, the components of point X are $\frac{2\pi}{a}(\frac{1}{2}, \frac{1}{2\sqrt{3}})$. Finally, triangle (ΓJX) being right-angled on X , one may write $\Gamma X^2 + XJ^2 = \Gamma J^2$ and one deduces that point J has components $\frac{2\pi}{a}(\frac{2}{3}, 0)$. The area of the triangle (ΓJX) is the irreducible Brillouin zone of the hexagonal Bravais lattice.